ORIGINAL ARTICLE

Cell Proliferation   WILEY

Abnormal microglial polarization induced by *Arid1a* deletion leads to neuronal differentiation deficits

Maolei Gong[1,2,3] | Ruoxi Shi[1,2,3,4] | Yijun Liu[1,2,3,4] | Jinpeng Ke[1,2,3,4] |
Xiao Liu[1,2,3] | Hong-Zhen Du[1,2,3] | Chang-Mei Liu[1,2,3,4] ⓘ

[1]State Key Laboratory of Stem Cell and Reproductive Biology, Institute of Zoology, Chinese Academy of Sciences, Beijing, China

[2]Institute for Stem Cell and Regeneration, Chinese Academy of Sciences, Beijing, China

[3]Beijing Institute for Stem Cell and Regenerative Medicine, Beijing, China

[4]Savaid Medical School, University of Chinese Academy of Sciences, Beijing, China

Correspondence
Chang-Mei Liu, State Key Laboratory of Stem Cell and Reproductive Biology, Institute of Zoology, Chinese Academy of Sciences, Beijing, China.
Email: liuchm@ioz.ac.cn

Abstract

Objective: Microglia, the prototypical innate immune cells of the central nervous system (CNS), are highly plastic and assume their phenotypes dependent on intrinsically genetic, epigenetic regulation or extrinsically microenvironmental cues. Microglia has been recognized as key regulators of neural stem/progenitor cells (NSPCs) and brain functions. Chromatin accessibility is implicated in immune cell development and functional regulation. However, it is still unknown whether and how chromatin remodelling regulates the phenotypic plasticity of microglia and exerts what kind of effects on NSPCs.

Methods: We investigated the role of chromatin accessibility in microglia by deleting chromatin remodelling gene *Arid1a* using microglia-specific Cx3cr1-cre and Cx3cr1-CreERT2 mice. RNA-seq and ATAC-seq were performed to dissect the molecular mechanisms. In addition, we examined postnatal M1/M2 microglia polarization and analysed neuronal differentiation of NSPCs. Finally, we tested the effects of microglial *Arid1a* deletion on mouse behaviours.

Results: Increased chromatin accessibility upon *Arid1a* ablation resulted in enhanced M1 microglial polarization and weakened M2 polarization, which led to abnormal neurogenesis and anxiety-like behaviours. Switching the polarization state under IL4 stimulation could rescue abnormal neurogenesis, supporting an essential role for chromatin remodeler ARID1A in balancing microglial polarization and brain functions.

Conclusions: Our study identifies ARID1A as a central regulator of microglia polarization, establishing a mechanistic link between chromatin remodelling, neurogenesis and mouse behaviours, and highlights the potential development of innovative therapeutics exploiting the innate regenerative capacity of the nervous system.

1 | INTRODUCTION

Microglia, the only resident immune cells that enduringly reside in the central nervous system (CNS),[1] play vital roles in regulating the homeostasis of CNS.[2] In the past years, studies on microglia have expanded from investigating their immunological functions as resident

macrophages of brain and mediators of neuroinflammation, injury, neurodegeneration to understanding their origins and functions involved in complex neurodevelopmental programs in the CNS.[3–6] Evidence has shown that microglia modulate neurogenesis and synaptic pruning, during which they interact with neural stem/progenitor cells (NSPCs) or neurons to provide trophic support, respond to

cytokines and drive the refinement of differentiation or maturation of precursors into neurons.[7] The role of microglia appears to be a double-edged sword in the battle for CNS damage and neurological recovery. Microglia activation acts as defender of the brain by resolving local inflammation, clearing cell debris, and releasing trophic factors[8,9] whereas microglia activation can also incumber neurogenesis and exacerbate tissue damage.[10–12] However, how to control or balance microglia activation and its subsequent effects on other cells in CNS are largely unknown.

Recent research has shown that microglia can harbour different phenotypes depending on intrinsic and extrinsic signals. Like microphages, microglia have three typical phenotypes, including two polarization types (M1 and M2) and a resting type (M0).[13] Under different stimulus, microglia could be activated into M1 and M2 polarized states. However, the mechanisms leading to their activation toward a specific phenotype and the reversibility of microglia polarization are not yet fully established. Microglia are involved in many brain disorders; however, little is known about how intrinsic or extrinsic signals impact microglial phenotype switch and function.

Chromatin remodelling, modulated by chromatin remodelers, is the rearrangement of chromatin from a condensed state to a transcriptionally accessible state, allowing transcription factors or other DNA-binding proteins to access DNA and control gene expression.[14] As a kind of M1 microglia inducer, LPS can switch microphage/microglia polarization. Gene loci analysis of LPS-inducible genes reveals particular requirements for SWI/SNF-dependent nucleosome remodelling in the transformation of microglia polarization.[15,16] The evolutionarily conserved multi-protein SWI/SNF complex, one of the largest chromatin-remodelling complexes, plays a critical role in coordinating chromatin architecture and gene expression.[17] Importantly, emerging remodelling in chromatin landscape, particularly enhancer landscape, plays an important role in macrophage polarization.[18–20] ARID1A, the largest subunit of the multi-protein SWI/SNF chromatin remodelling complex,[21] assembles with either BRM or BRG1 to form a functional chromatin-remodelling complex.[22] *Arid1a* has a dominant role in maintaining chromatin accessibility at enhancers,[23] acting as an important regulator of most essential neurogenic genes during early neural development.[24] Notably, *Arid1a* mutation is correlated with altered expression of various genes and gene sets involved in the immune response,[25] which indicates that *Arid1a* may have function in immune cells. Human genetic studies have identified dysregulation of ARID1A in Coffin-Siris syndrome (CSS), a congenital disorder characterized by intellectual disability and growth deficiency.[26] Furthermore, early-life inflammation and the potential roles for microglia have been documented in immune-driven animal models of autism and schizophrenia.[27] These studies, together with our previous data showing that *Arid1a* has a high expression in microglia cells in CNS,[28] suggesting a potential role for *Arid1a* in microglia and inflammation phenotypes observed in neurodevelopmental disorders. However, there are no animal models available to study the direct role for Arid1a in the modulation of microglia phenotypes.

Here, we established a conditional allele to manipulate cell-type-specific *Arid1a* function in CNS microglia. We found that *Arid1a* loss in microglia prior to birth led to abnormal polarization, which then resulted in enhanced M1 microglial polarization and weakened M2 polarization. Importantly, microglial polarization anomaly induced by absence of *Arid1a* led to abnormal neurogenesis and anxiety-like behaviour. We further identified microglia M2 phenotype inducer interleukin-4 (IL-4) could stimulate the switch of microglia polarization and restored abnormal neurogenesis. Collectively, our results demonstrate a critical role for ARID1A in the development of microglia and neuronal differentiation, which provides insights into the genetic basis and potential therapeutic interventions of ARID1A-related intellectual disabilities such as Coffin–Siris syndrome.

2 | MATERIALS AND METHODS

2.1 | Mice

All animal experiments were approved by Laboratory Animal Center, Institute of Zoology, Chinese Academy of Sciences, and were performed in accordance with the respective national regulations of China. The *Arid1a*^{fl/fl} mouse[29] was a kind gift from Dr Zhong Wang (Harvard Medical School). To generate microglia-specific Arid1a deleted animals, we crossed *Arid1a*^{fl/fl} mouse with either Cx3cr1-Cre (JAX Stock No. 005628) or Cx3cr1-CreERT2 (JAX Stock No. 020940) line. To get the iKO mice line, 8 mg of Tamoxifen (TAM, Sigma-Aldrich) dissolved in corn oil was applied by intraperitoneal injections to mice from P0 to P5. All mice were bred in specific-pathogen-free facility with a 12 h light/dark cycle. Mice genotypes were performed by PCR assay using tail genomic DNA. Genotyping primers are listed in Table S2 (Supplementary Information). All procedures were approved by Animal Committee of Institute of Zoology, Chinese Academy of Sciences.

2.2 | Primary cell culture

For NSPCs, forebrain from P7 pups was freed from meninges and washed in phosphate buffer saline (PBS) with gentle trituration followed by centrifugation at 400*g* for 10 min. Next, brain tissues were digested with TrypLEME Express (Gibco, 12,604,013) at 37°C for 10 min. Neurobasal™ Medium containing 10% FBS (Gibco, 10,099,141), 1% GlutaMAX (Gibco, 35,050,061) and 1% Penicillin–Streptomycin (Hyclone, SV30010) was added into each digestion product to stop digestion. After repetitive pipetting, cell suspension was passed through 70-μm cell strainer, and then was cultured with Neurobasal™ Medium containing N2 supplement (0.5%, GIBCO) and B27 (0.5%, GIBCO), Penicillin–Streptomycin (1%, Hyclone), fibroblast growth factor-2 (20 ng/ml, PeproTech), and epidermal growth factor (20 ng/ml, PeproTech) in a 5% CO_2 incubator at 37°C. For differentiation of NSCs, NSCs were first seeded on poly-L-ornithine/laminin-coated coverslips at a density of 1×105 cells/well. NSCs were incubated with DMEM/F-12 medium containing N2 supplement and B27, Penicillin–Streptomycin, forskolin (5 μM, Sigma-Aldrich), and retinoic acid (5 μM, Sigma-Aldrich) for 3 days.

For microglia, cortical hemispheres from newborn mice (P0-3) were freed from meninges, and digested with TrypLEME Express at 37°C for 10 min. And then, cell suspension was plated in 25 cm^2 tissue culture flasks with DMEM/F12 supplemented with 10% FBS. After a 2 weeks culture, the flasks were shaken for 2 h at 130 rpm to harvest microglia. For microglia and NSPCs co-culture, 2000 microglia were seeded on a single well of 24-well plate for 24 h, 50 ng/mL Il4 was added if needed, following with 10^5 NSPCs planting. When the secretion function was done, 2000 microglia was seeded over 0.4 μm trans well, and 10^5 NSCs blow.

2.3 | BrdU incorporation analysis

Based on the mouse weight, intraperitoneal injection was used to inject pregnant mice at day 18.5 with 100 mg/kg BrdU (Sigma, B5002-5G). The brains were harvested at P7 and P14 for the following analysis.

2.4 | Flow cytometry

Mice were anaesthetized with avertin (sigma) and transcardially perfused with ice-cold PBS. The tissue was digested using a Papain Dissociation System kit (Worthington, LK003150) following the manufacturer's recommendations. Cell suspension was collected and washed extensively with fluorescence activated cell sorter (FACS) buffer (2% FBS in PBS) followed by staining with anti-CD11b APC (clone M1/70, Biolegend) and anti-CD45 PE (clone 30-F11, Biolegend) for microglia isolation, and anti-mouse CD16/32 APC/cy7 (clone 93, Biolegend) and anti-mouse CD206 FITC (clone c068c2, Biolegend) for polarization analysis.

2.5 | RNA-seq, ATAC-seq and ChIP-seq analysis

The total RNA was extracted from FACS sorted WT or cKO microglia according to procedures with TRIzol reagent (Invitrogen, 15596018). A 2 μg RNA was used for sequencing libraries generation using NEB-Next® Ultra™ RNA Library Prep Kit for Illumina® (#E7530L, NEB, USA) following the manufacturer's recommendations. The cDNA library was analysed by Illumina HiSeq 2500 platform. After that, the library was measured using Qubit® RNA Assay Kit in Qubit® 3.0 to preliminary quantify and then dilute to 1 ng/μl. Insert size was assessed using the Agilent Bioanalyzer 2100 system (Agilent Technologies, CA, USA), and qualified insert size was accurate quantification using StepOnePlus™ RT PCR. The clustering of the index-coded samples was performed on HiSeq PE Cluster Kit v4-cBot-HS (Illumina), and the libraries were sequenced on an Illumina platform. Finally, 150 bp paired-end reads were generated with help of Annoroad Gene Tech. (Beijing) Co., Ltd. The RNA-seq data are available in Sequence Read Archive (SRA) under BioProject PRJNA812340.

For ATAC-seq, 50,000 primary microglia were taken for library preparation. The cells were lysed in Lysis Buffer (10 mM NaCl, 3 mM MgCl2, 0.15% NP-40, in pH 7.410 mM Tris–HCl) to get the nuclei, and TruePrep™ DNA Library Prep Kit V2 for Illumina (Vazyme Biotech, TD501) was used to construct the transposase-treated libraries. Qubit 3.0 Fluorometer and StepOnePlus™ real-time PCR system used for the mass concentration and molar concentration of libraries analysis, respectively. Agilent HS 2100 Bioanalyzer was used to detect the lengths of inserted fragments. Qualified libraries were sequenced by Illumina HiSeq X 10 platform in pair-end 150 bp style with the help of Annoroad Gene Tech. (Beijing) Co., Ltd. The ATAC-seq data are available in SRA under BioProject PRJNA812630.

For ChIP-seq, the Chip-seq data for *Arid1a* was downloaded from SRA under BioProject PRJNA638150.[30]

2.6 | Western blot analysis and RT-PCR

Total RNA from FACS sorted or primary microglia was reverse transcribed into cDNA using Transcript One-Step gDNA Removal and cDNA synthesis Kit (TransGen Biotech, Beijing, China). Then, cDNA was quantified by using Hieff® qPCR SYBR® Green Master Mix (Yeasen Biotech, 11201ES08). The analysis of relative gene expression was executed by the $2^{-\Delta\Delta CT}$ method, and actin was used as endogenous control. RT-PCR primers are listed in Table S1 (Supplementary Information).

The total protein of primary microglia was extracted using RIPA buffer containing 10 mM PMSF (Beyotime Biotechnology, ST505), and the concentration of it was defined using BCA protein assay kit (Beyotime Biotechnology, P0012). The membranes were blocked in 5% milk in TBS-T (0.1% Tween 20) and incubated with the primary antibodies, including Anti-beta Tubulin (1:5000, Abcam) and anti-Arid1a (1:2000, Sigma) at 4°C overnight. The membranes were then washed in TBS-T for 10 min × 3 times, and then incubated with the secondary antibodies at room temperature for 2 h. ECL system (Pierce) and Tanon-5200 Chemiluminescent Imaging System (Tanon, China, Shanghai) was used for signal detection conducting.

2.7 | Immunofluorescence staining

The brain isolated from perfused mice was post-fixed with 4% paraformaldehyde (PFA) overnight, and dehydrated with 30% sucrose later. The tissue was used for cryo embedding, and cut into 35-μm-thick cryosections. For primary cells, cultured cells were seeded on coverslips and fixed with PFA. To get immunofluorescence analysis results, sagittal brain slices or coverslips were permeabilized (0.5% Triton X-100, 3% BSA in PBS) for 15 min and blocked (0.3% Triton X-100, 3% BSA in PBS) for 1 h at room temperature, first. Next, slices were incubated with the relevant primary antibodies (0.3% Triton X-100, 3% BSA in PBS) overnight at 4°C, including anti-Arid1a (1:500, Sigma), anti-Iba1 (1:500, Wako), anti-Tuj1 (1:1000, Biolegend), anti-GFAP (1:500, Abcam), anti-BrdU (1:500, Abcam), anti-NeuN (1: 1000, Millipore) and Anti-Doublecortin (1:500, Abcam). Alexa Fluor 488, 568, 594 or 647 secondary antibodies (1:500, Life Technologies) were

used for corresponding staining, and Nuclei were counterstained with DAPI (1:1000, Sigma).

2.8 | Microscope imaging and three-dimensional reconstruction of microglia

Confocal images were acquired using Zeiss LSM880 confocal microscopes and analysed by ZEN software. Three-dimensional (3D) surfaces were reconstructed using the IMARIS surface reconstruction tool depending on Iba1 immunofluorescence staining.

2.9 | Behaviour tests

2.9.1 | Open field

Open-field testing was conducted using 6–8 –week-old male mice in a 33 cm × 33 cm × 40 cm box for 15 min, and total distance, average speed, time spend in the centre, and entrance times of the centre were quantified by Smart 3.0 during the first 10 min. The centre zone was marked as a 14 cm square.

2.9.2 | Light–dark box testing

The light–dark box (LDB) was made of white and black opaque Plexiglas (20 cm × 30 cm × 30 cm light chamber, 30 cm × 30 cm × 30 cm dark chamber). The chambers were connected by a 10 × 10 cm door in the middle of the wall separating the two chambers. Animals were placed in the middle of the dark box for 3 min facing a side away from the door and then released. LDB was conducted for 8 min with time in the light box and light box entries calculated with Smart 3.0 during the first 5 min. Mice were used as in Open field.

2.9.3 | Elevated plus maze

Elevated plus-maze testing was conducted for 8 min with time in the open arm and open arm entries calculated with Smart 3.0 during the first 5 min. Mice were used as in Open field.

2.9.4 | Morris water maze test

A circular water tank (diameter = 120 cm) was filled with water, and the water was made opaque with non-toxic white paint. A round platform (diameter = 13 cm) was hidden 1 cm beneath the surface of the water at the centre of a given quadrant of the water tank. Mice received training in the Morris water maze for 6 successive days; each session consisted of 4 trials. A probe test was conducted 24 h after completion of the training. During the probe test, the platform was removed from the pool, and task performance was recorded for 60 s.

2.9.5 | Fear conditioning test

Prior to the experiment, mice were handled for 5 min per day for 3 consecutive days. During training, mice explored context A (grid floor with transparent cage walls) for 2 min, then received one pairing of a tone (amplitude 85 dB for 30 s) co-terminated with a foot shock (0.6 mA, 1 s). Contextual fear was tested 24 h after conditioning by placing the animals in the conditioning context (context A) for a 5-min period. For auditory fear conditioning, the test consisted of a 2-min acclimatizing period to the context B (grid floor and cage walls were covered with yellow plastic to create another context), followed by a 3-min period during which the tone was delivered (CS).

2.9.6 | Marble burying test

A large cage (45 cm × 22 cm) with transparent filter tops filled with 5 cm of fresh and compact corncob bedding and 4 × 6 marbles (diameter = 2.3 cm) that were equally distributed along the walls. Mice were placed in the middle of the cage and left undisturbed for 30 min. Finally, the number of marbles, which more than 2/3 of their volume was buried, was counted. Mice were used as in Open field.

2.9.7 | Self-grooming test

The self-grooming task consisted of an initial 10 min of habituation, followed immediately by a 10 min measure of self-grooming. Mice were singly placed in plastic containers (45 cm × 22 cm). Grooming time was recorded in seconds, and self-grooming behaviour included obvious self-grooming on genital, tail, paw, leg, body and head.

2.10 | Statistical analysis

Data are represented as mean ± SEM, unless otherwise indicated. Experiments were conducted in at least 3 biological replicates ($n \geq 3$) for each group. For statistical analyses, unpaired Student's t-tests were executed using GraphPad Prism software. Statistical significance was defined as $*p < 0.05$, $**p < 0.01$, $***p < 0.001$, $****p < 0.0001$.

3 | RESULTS

3.1 | *Arid1a* ablation enhances microglial chromatin accessibility and alters transcriptomic profile

The *Arid1a* gene, which encodes a subunit of the SWI/SNF chromatin remodelling complex, has an ARID domain considered to facilitate non-specific DNA binding.[31,32] To study the function of *Arid1a* and assess the effects of *Arid1a* ablation on chromatin accessibility in microglia, we first generated *Arid1a*^{fl/fl};Cx3cr1-cre mice line by

crossing *Arid1a*^{fl/fl} with Cx3cr-cre transgenic mice to delete *Arid1a* specifically within microglia in brain (Figure S1A). We isolated primary microglia from *Arid1a*^{fl/fl};Cx3cr1-cre⁺ (cKO) and the corresponding control *Arid1a*^{fl/fl};Cx3cr1-cre⁻ (WT) mice. Compared to WT, the absence of *Arid1a* in microglia was first validated by quantitative real-time RT-PCR (Figure 1C) and western blotting (Figure 1D, E). And similarly, cKO microglia has none localized ARID1A in nucleus as shown in immunostaining (Figure 1F), indicating that *Arid1a* was deleted.

We then analysed chromatin accessibility with ATAC-seq in primary *Arid1a* cKO and WT microglia. Our results showed that cKO microglia dramatically altered overall chromatin accessibility compared to WT (Figure 1A and Figure S1G). The alterration of chromatin accessibility in microglia impaired transcriptomic profile of microglia isolated from cKO as compared with WT based on microglial RNA-seq analysis (Figure 1B).

3.2 | Enhanced chromatin accessibility in microglia lacking *Arid1a* results in microglial malformation

Enrichment analysis supported strong up-regulation of gene ontologies (GO) such as negative regulation of cell cycle (GO:0045786), negative regulation of cell cycle process (GO:0010948), and negative regulation of chromosome segregation (GO:0051985, Figure 1G), which confirmed the results that *Arid1a* absence led to decreased proliferation of microglia. We then analysed the impact on microglia by using IBA1 as a microglia marker in the mouse hippocampus and cortex (Figure 1H). The quantification result showed that there was an increased number of cells expressing Iba1 in cKO mice compared to WT at postnatal day (P) 9, 14, 21 and 56 (Figure 1I). To confirm that, we then generated *Arid1a*^{fl/fl};Cx3cr1-creERT2 mice and induced *Arid1a* deletion with tamoxifen (TAM) injection starting from P0 (Figure S1B). The cortical and hippocampus microglia also demonstrated a significant decrease of cell number after TAM injection at P14 (Figure S1C–E). IMARIS-based 3D morphometric measurements of microglia further revealed that microglia exhibited shorter processes and reduced numbers of terminal points at P14 (Figure 1J-K). These data suggested that *Arid1a* is indispensable for proliferation and structural construction of microglia.

## 3.3 | *Arid1a* absence results in enhanced M1 microglial polarization and decreased M2 polarization

Based on our RNA-seq analysis, we found that *Il1a* expression increased significantly upon *Arid1a* deletion (Figure 1B, black arrow). The enhancement of *Il1a* expression is considered as a marker for microglia M1 polarization,[33] suggesting that *Arid1a* ablation may result in abnormal microglia polarization. To directly assess the function of *Arid1a* in microglial polarization, we analysed the expression of microglial genes involved in polarization (Figure 2A, *padjust* < 0.05, log2foldchange >1.5). The RNA-seq results showed that M1 microglial genes, including *Ki*, *Tlr*, *Il1a*, *Il1b*, *Il6*, *Il18* and *Tmem47* significantly

increased (Figure 2B, middle). In contrast, M2 microglial genes, including *Igf1*, *C1qa*, *Arhgap22*, *Tim47*, *Timp2*, *sema6d* and *fgd2*, significantly decreased (Figure 2B, right). However, M0 microglial genes remained unchanged (Figure 2B, left). This gene expression pattern was confirmed further by qRT-PCR (Figure 2C–E). Moreover, we used FACS analysis and identified the polarization states of microglia isolated from cKO and WT mice at P14 by M1/M2 labelled antibodies (Figure 2F). The results demonstrated that the ratio of Cd16/32 positive cells (M1) in Cd45^{low}&Cd11b^{high} cells markedly increased (Figure 2G, left), but the ratio of Cd206 positive cells (M2) decreased (Figure 2G, right). Collectively, these results indicated that loss of *Arid1a* altered the balance of microglial M1/M2 polarization, suggesting an essential role for ARID1A in the phenotypic plasticity of microglia.

3.4 | Enhanced chromatin accessibility in microglia lacking *Arid1a* dysregulates neurogenesis

Recent studies indicate that microglial polarization has important effects on neurogenesis,[10,34] during which M1 microglia inhibits and M2 microglia promotes neurogenesis.[35] In our microglia-specific *Arid1a* ablation mouse model, we found abnormal M1/M2 polarization, as well as alterations of gene expression were involved in neurogenesis. Based on GO enrichment, we found that *Arid1a* loss in microglia can affect neurons supported by significant up-regulation of negative regulation of neuronal differentiation term (GO:0045665), and negative regulation of nervous system development (GO:0051961), indicating that microglial *Arid1a* ablation may cripple neurogenesis (Figure 3A).

To test the hypothesis that microglia polarization anomaly induced by *Arid1a* deletion may cripple neurogenesis, we first quantified differentiated neurons by NeuN immunofluorescence (Figure 3B). The results showed that the number of neurons markedly decreased in the cortex (Figure 3C, left) and hippocampus of cKO mice (Figure 3C, right). To investigate whether the decrease of neurons was caused by deficient neurogenesis upon *Arid1a* loss in microglia, we injected mice with BrdU at E18.5 to label proliferative NSPCs and then analysed the newly generated neurons after birth. BrdU, Doublecortin (DCX) and NeuN immunofluorescence staining was used to label the cell identity (Figure 3D). The quantification results showed that, compared to WT, both the immature neurons (BrdU⁺ DCX⁺) (Figure 3D, white arrows with tails) and mature neurons (BrdU⁺⁻ NeuN⁺) (Figure 3D, white arrows without tails) that differentiated from NSPCs dramatically decreased at P7 and P14 (Figure 3E, F). To further verify the defects of neurogenesis observed in cKO mice, we co-cultured primary NSPCs with primary microglia isolated from P7 mice and analysed the differentiation abilities of NSPCs (Figure 3G). Compared to WT, NSPCs co-cultured with cKO microglia differentiated into fewer neurons (Figure 3H), but astrocytes differentiation was not affected (Figure 3I). Moreover, compared to WT, NSPCs co-cultured with cKO microglia did not alter proliferation efficiency of NSPCs (Figure S1I-J), but enhanced cell apoptosis (Figure S1K-L).
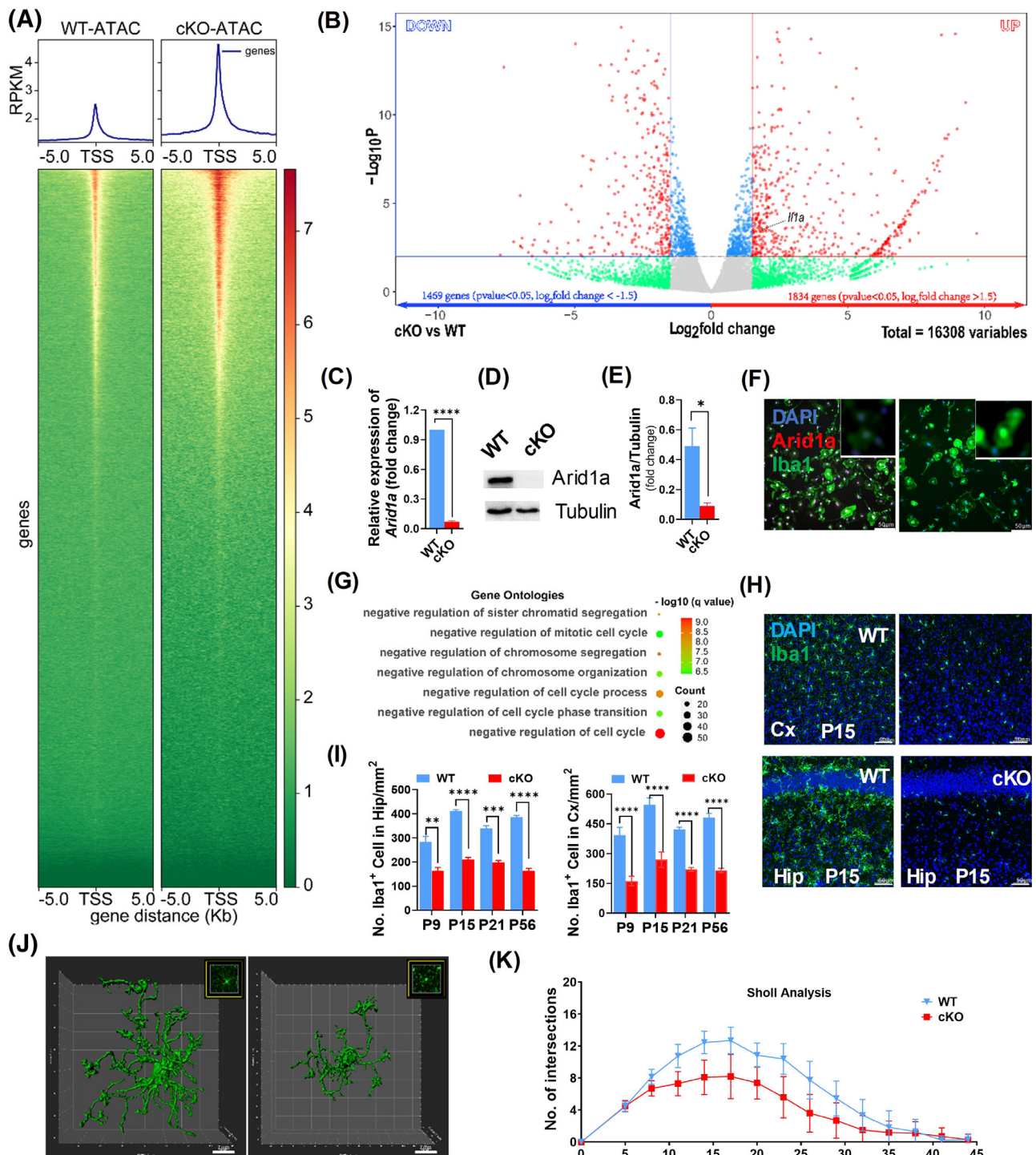
FIGURE 1 Absence of *Arid1a* Alters Microglial Chromatin Accessibility, Transcriptomic Profile and Development. (A) Average profile of ATAC-seq signal in *Arid1a* cKO microglia compared to WT, plotted within $+/-$ 5 kb of transcription start site (TSS, down) and fragments per kilo base of transcript per million mapped fragments (PRKM, up) of NCBI-annotated genes. (B) Example volcano plot. Points on top-right and top-left corners are considered the most promising genes ($p < 0.05$, log2foldchange >1.5) in 16,308 significantly changed genes. (C–E) Expression of *Arid1a* in primary microglia cells. Total RNAs (C) and protein (D) were extracted from WT and cKO primary microglia and tested with RT-PCR and western blotting and the expression of Arid1a protein level was quantified in (E). (F) Arid1a staining in cultured primary microglia isolated from WT and cKO. (G) Pathway analysis of cell cycle-related affection based on gene ontology (GO) database. Count means number of genes involved in the specific pathway. (H–I). Representative image (H) and Quantification (I) of microglia in cortex and hippocampus. Iba1 was used for frozen section staining collected at day 9, 15, 21, 56 after birth. (J, K) Morphology of microglia in WT and cKO. Three-dimensional (3D) surfaces of microglia were reconstructed using the IMARIS surface reconstruction tool depending on Iba1 immunofluorescence staining (J), and the sholl analysis was analysed using ImageJ and the results were shown in (K). Data are expressed as mean ± SEM and analysed by Student's *t*-test from at least three independent experiments. *$p < 0.05$, **$p < 0.01$, ***$p < 0.01$ and ****$p < 0.01$
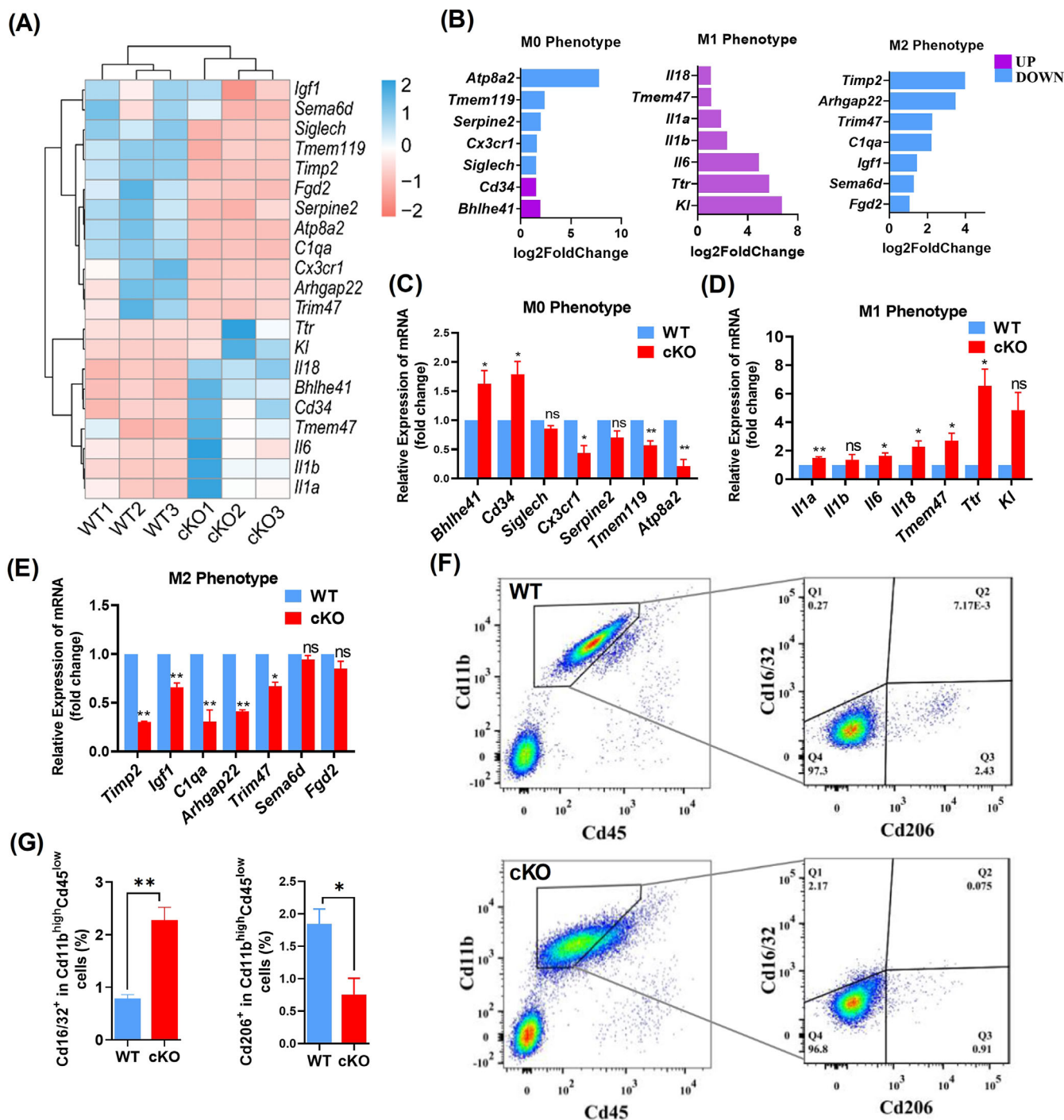
FIGURE 2 *Arid1a* absence results in enhanced M1 type polarization. (A) Hierarchical clustering of microglial polarization-related genes which are significantly altered ($p < 0.05$, log2foldchange >1.5) in cKO microglia of P14 mice in RNA-seq analysis ($N = 3$), compared to WT. The heatmap displays z-transformed expression values. (B) Log2foldchange of microglial polarization-related genes ($p < 0.05$), which are significantly changed between microglia from cKO and WT mouse at P14 obtained from RNA-seq analysis. (C) Expression of M0 microglia marker genes. The expression of these genes was examined at mRNA levels using RT-PCR, β-actin was used as a standard control. Total RNA was extracted from cKO and WT microglia isolated through FACS. (D). Expression of M1 microglia marker genes. (E) Expression of M2 microglia marker genes. (F, G) Flow cytometric characterization of microglia in P14 mice. Cd45 PE and Cd11b APC antibodies were used for microglia identification, Cd16/32 APC/Cy7 and Cd206 FITC anti-mouse specific antibodies were used for M1 or M2 microglial identification, respectively (F), the ratio of M1 or M2 in total microglia was analysed by the number of Cd16/32$^+$ or Cd206$^+$ cells per the number of Cd45^{low}Cd11b^{high} cells (G). Data are expressed as mean ± SEM and analysed by Student's *t*-test from at least three independent experiments, *$p < 0.05$ and **$p < 0.01$
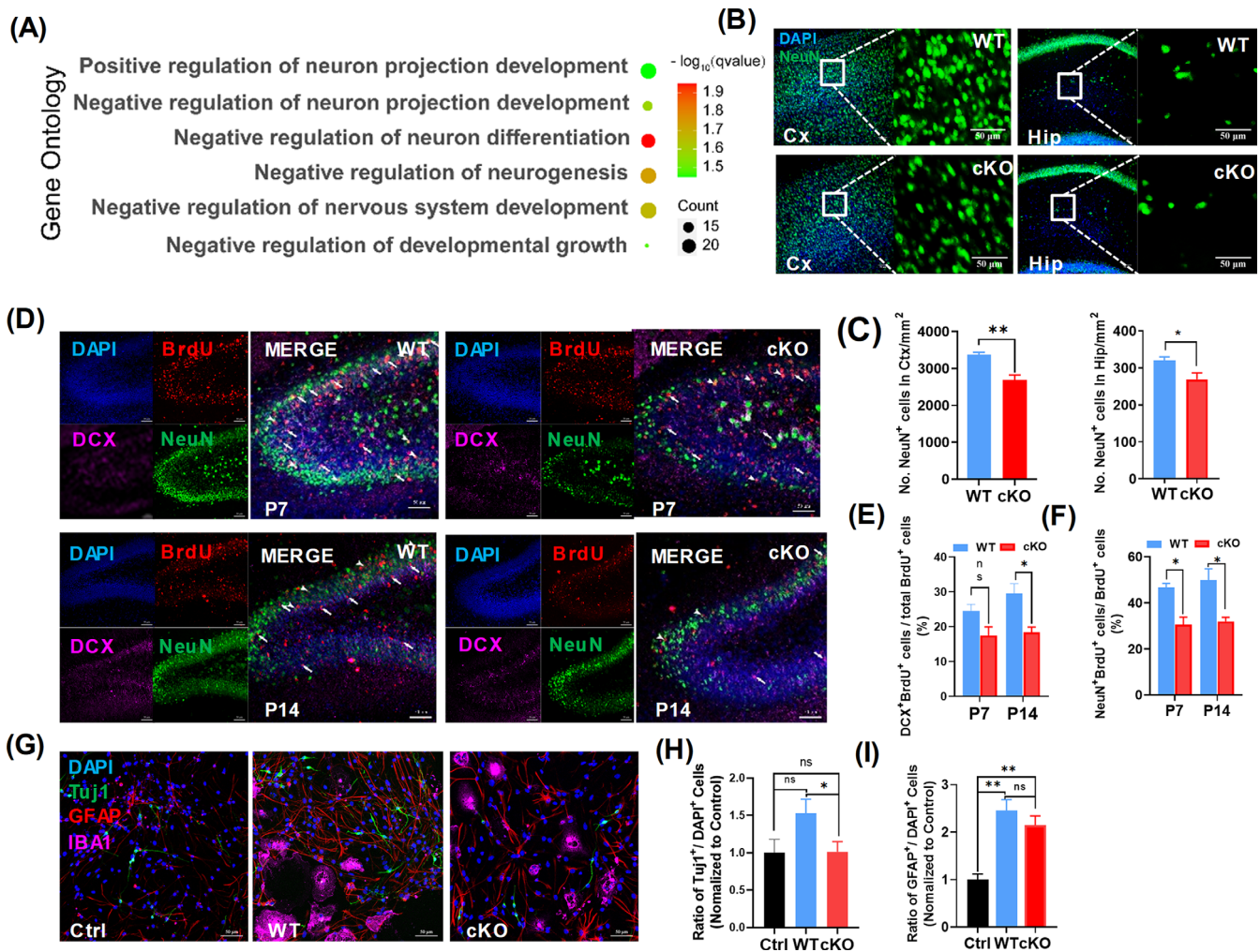
FIGURE 3 Absence of microglia *Arid1a* during development inhibits neuronal differentiation. (A) Pathway analysis of neuro-related affection based on gene ontology (GO) database. Count means number of genes involved in the specific pathway. (B, C) Cortex and hippocampus NeuN staining in *Arid1a* cKO and WT mice. Immunofluorescence staining was performed in frozen section of 14-day-old mice using NeuN antibody (B), and the number of neurons in cortex and hippocampus (C) were quantified by NeuN$^+$ cells per square millimetre, respectively. (D–F) Hippocampal DG area staining of *Arid1a* cKO and WT mouse. Immunofluorescence staining was performed in frozen section of 7- or 14-day-old mice using specific antibodies BrdU, DCX and NeuN (D), BrdU was injected at E18.5 and the number of neurons differentiated from neural stem/progenitor cells (NSPCs) were quantified by DCX$^+$Brdu$^+$ (E) or NeuN$^+$Brdu$^+$ (F) cells in BrdU$^+$ cells. (G–I) Differentiation test of NSPCs in vitro. Total of 100,000 NSPCs from WT mice were co-cultured with 20,000 cKO or WT microglia for NSPCs differentiation, specific antibodies for Iba1, Tuj1 and GFAP were used for analysis of NSPCs differentiation (G), and the percentage of differentiated neurons (H, Tuj1$^+$ cells) and astrocyte (I, GFAP $^+$ cells) were showed. Scale bar = 50 μm. Data are expressed as mean ± SEM and analysed by Student's *t*-test from at least three independent experiments, *$p < 0.05$ and **$p < 0.01$

Together, these data provide strong support of an essential role for ARID1A in maintaining the balance of microglia polarization and promoting neurogenesis.

3.5 | *Arid1a* modulates *Il-1a* expression and affects neuronal differentiation of NSPCs

Phagocytosis and secretion are the most basic functions of microglia.[36] To determine whether *Arid1a* ablation affects gene expression associated with the fundamental functions of microglia, such as

phagocytosis and secretion, we performed top 20 kyoto encyclopaedia of genes and genomes (KEGG) analysis. The results revealed that the differentially up-regulated genes (*padjust* <0.05, log2foldchange >1.5) in cKO microglia were enriched in 4 pathways related to cell secretion, including cytokine-cytokine receptor interaction (mmu04060), inflammatory bowel disease (mmu05321), haematopoietic cell lineage (mmu04640) and cellular senescence (mmu04218, Figure 4A). Combined gene network analysis further demonstrated that *Il1a* (interleukin 1 alpha) and *Il6* (interleukin 6) were involved in all these 4 pathways (Figure 4B, black arrows). Genome-browser view of ATAC-seq showed a significant peak gain of *Il1a*
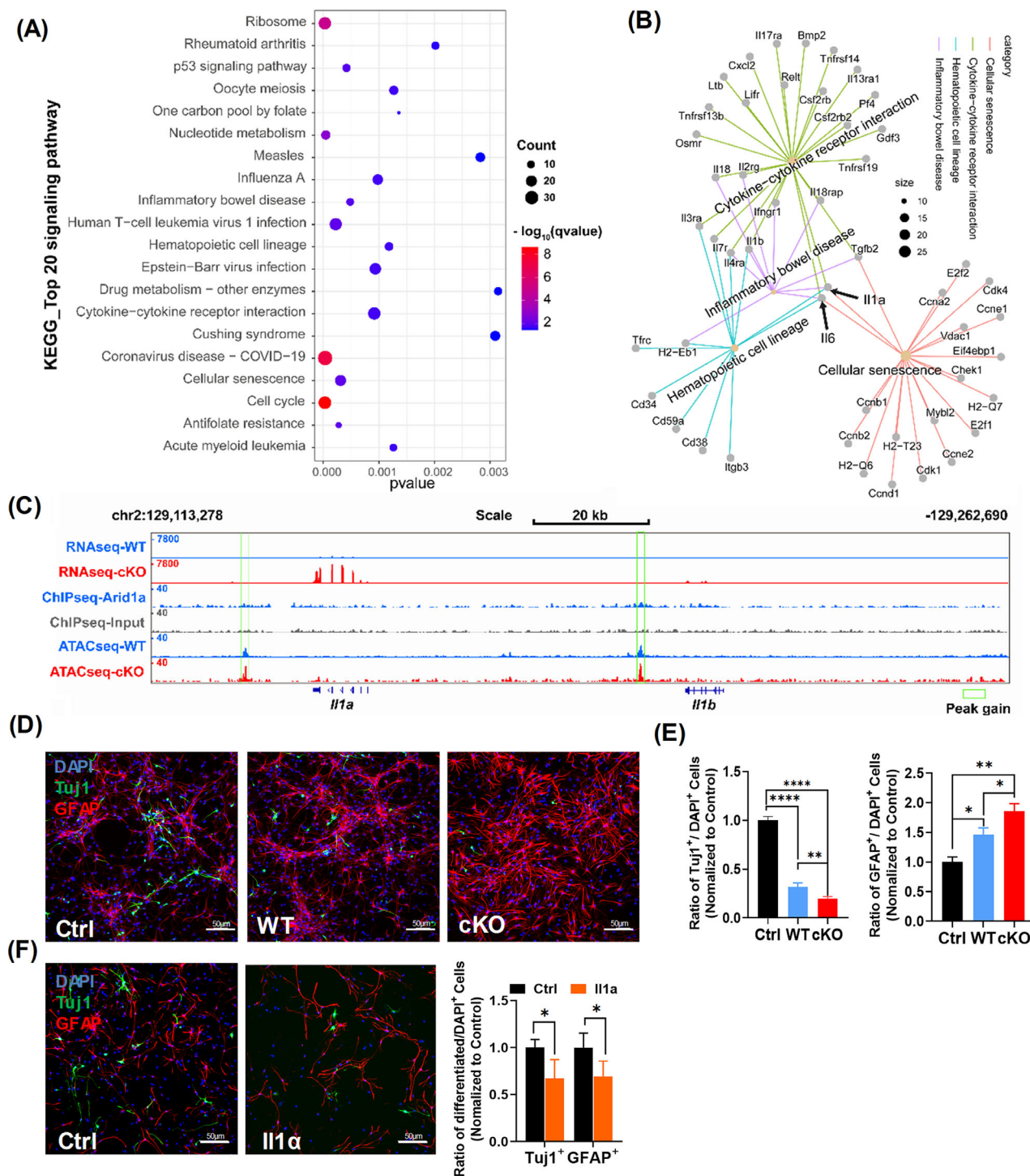
FIGURE 4 *Arid1a* Modulates Il1a Expression and Affects Neuronal Differentiation of neural stem/progenitor cells (NSPCs). **(A)** Top 20 pathway analysis based on KEGG database revealing the differentially expressed genes ($p < 0.05$, log2foldchange >1.5) in cKO microglia were enriched for multiple cellular biological processes, count means number of genes involved in the specific pathway. (B) Cellular secretion-related KEGG pathway gene network analysis, including cytokine–cytokine receptor interaction, inflammatory bowel disease, cellular senescence and haematopoietic cell lineage. Size means number of genes involved in the specific pathway, the black arrow points to the genes involved in all these pathways above, including *Il6* and *Il1a*. (C). Genome-browser view of RNA-seq ($n = 3$), ChIP-seq ($n = 1$), and ATAC-seq ($n = 2$) at *Il1a* and *Il1b*, the green rectangle was used for pointing out the peak gain. (D) NSPCs differentiation using microglia and NSPCs contactless culture system and 0.4 μm trans well were used. For NSPCs differentiation, 20,000 cKO or WT microglia were seeded on the upper side of the trans well membrane and 100,000 NSCs from WT mice were seeded on the lower side, and specific antibodies for Tuj1 and GFAP were used for analysis of NSPCs differentiation. (E) Quantification of Tuj1 and GFAP positive cells ($n = 3$). (F) Il1a-stimulated NSPCs differentiation. Left, representative images of Tuj1 and GFAP staining. Right, quantification of Tuj1 and GFAP positive cells ($n = 3$). Data are expressed as mean ± SEM and analysed by Student's *t*-test from at least three independent experiments. *$p < 0.05$, **$p < 0.01$, and ****$p < 0.0001$

(Figure 4C), but not *Il6* (Figure S1 H). To further analyse whether *Arid1a* could directly regulate *Il1a* expression，we downloaded the deposited *Arid1a* ChIP-seq data.[30] The analysed data demonstrated that ARID1A has enrichment on the site where *Il1a* showing a significant peak gain after *Arid1a* deletion in our ATAC-seq, suggesting that ARID1A could directly regulate *Il1a* expression (Figure 4C). Taken together, these data indicated that microglial abnormality in the absence of *Arid1a* during development affected neuronal differentiation and cytokines secretion.

As we showed above, cytokines secretion may play an important role in ARID1A-mediated functions in microglia (Figure 4A). Unlike cell-to-cell connections, paracrine does not need direct contact between cells. We then asked whether paracrine of microglia mediates the deficiency of *Arid1a* cKO NSPCs in neuronal differentiation. We established microglia and NSPCs contactless culture system with 0.4 μm trans well. The differentiation of NSPCs seeded on the lower side was analysed using immunofluorescent staining (Figure 4D). Compared to WT, cKO NSPCs significantly reduced neuronal differentiation (Figure 4E, left) and enhanced astrocyte differentiation (Figure 4E, right). Given that we observed a significant up-regulation of gene expression and chromatin accessibility of *Il1a* in *Arid1a* cKO microglia, we then investigated whether ARID1A promotes neuronal differentiation through Il1a secretion. By directly adding recombinant mouse Il1a to the cultured primary NSPCs with neuronal differentiation medium (Figure 4F, left), we found that Il1a treatment decreased neuronal differentiation in cultured NSPCs (Figure 4F, right). These results indicated that *Arid1a* ablation in microglia causes neuronal differentiation defects likely through Il1a overexpression.

3.6 | Il4-stimulated switch of microglia polarization corrects neuronal differentiation defects

Last, we assessed whether switch of irregular microglia polarization from M1 to M2 could correct neuronal differentiation deficiency caused by *Arid1a* deletion in microglia. We used Il4, which has been demonstrated to stimulate M2 polarization,[35] to culture microglia in vitro. RT-PCR results showed significant enhancement of M2 microglial polarization with increased expression level of *Arg1* and *C1q*, markers of M2 microglia, under Il4 stimulation (Figure 5A). Moreover, compared to Il4 free group, Il4-treated *Arid1a* cKO group demonstrated the recovery of neuronal differentiation (Figure 5B, C), which indicates that switching the abnormal microglial polarization states induced by *Arid1a* ablation in microglia is sufficient to reverse the deficiency of neuronal differentiation. Together, these findings demonstrate that the abnormal dynamic equilibrium of microglial polarization following *Arid1a* deletion is a key mechanism which mediates the defective neurogenesis and brain development in *Arid1a* cKO mice.

3.7 | Absence of microglial *Arid1a* prior to birth leads to anxiety-like behaviour in mice

Previous studies indicate that neurogenesis has significant correlation with emotion, especially depression and anxiety.[37,38] Abnormal neurogenesis causes behavioural impairments, including learning and memory.[39,40] What's more, evidence shows that defects of immune cells, including CD4+ T-cells, Th17/Treg, mast cell and microglia,[41-44] lead
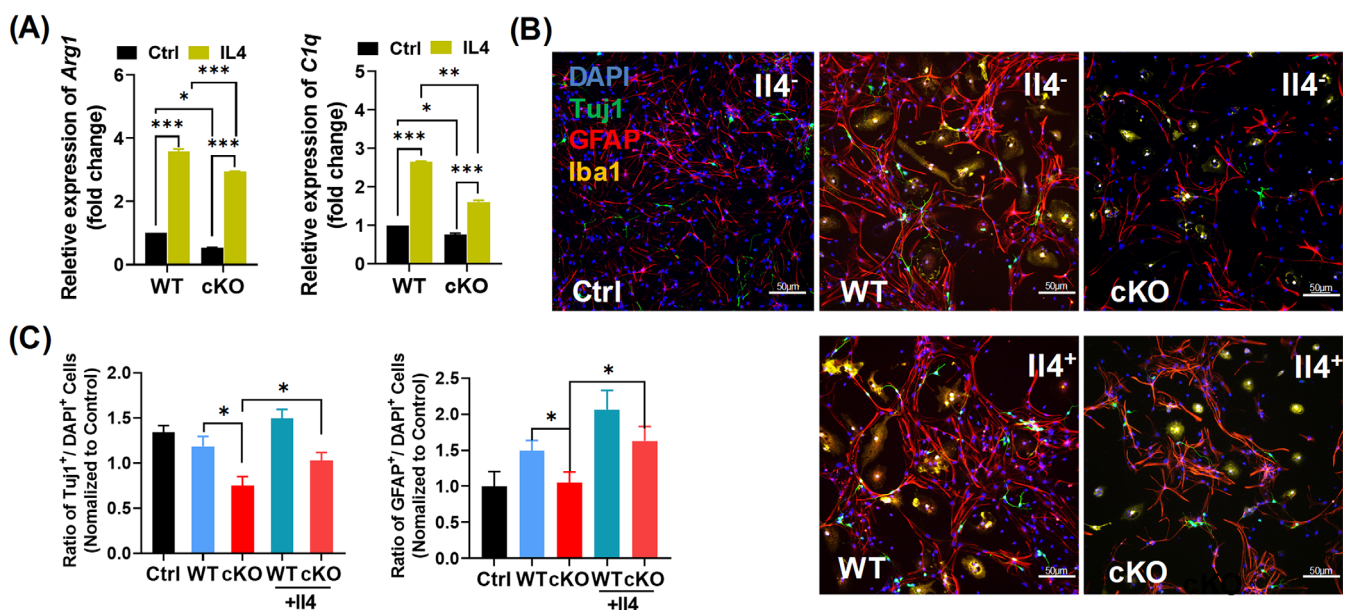

FIGURE 5 Switching microglia polarization corrects deficient neuronal differentiation. (A) The expression of Arg1 and C1q in WT and cKO microglia. Total RNA was extracted from Il4-stimulated Microglia, actin was used as an internal reference. (B) Differentiation of neural stem/progenitor cells (NSPCs) co-cultured with Il4-stimulated microglia in vitro. Iba1, Tuj1 and GFAP were used for analysis of NSPCs differentiation. (C) The ratio of differentiated neurons (left) and astrocytes (right) were shown. Scale bar = 50 μm. Data are expressed as mean ± SEM and analysed by Student's t-test from at least three independent experiments. *p < 0.05, **p < 0.01, ***p < 0.001

to mouse anxiety or anxiety-like behaviours. We then assessed whether the deficient neurogenesis caused by microglial *Arid1a* deletion could affect mouse behaviours. As revealed in open-field tests, although *Arid1a* cKO mice showed significant loss in body weight (Figure S2J), they had intact motor function (Figure 6A). First, we examined anxiety-like behaviours by performing open field, light–dark box tests, and elevated plus maze. The anxious mice tended to avoid open, exposed and brightly illuminated areas. The results demonstrated that *Arid1a* cKO mice spent less time in the centre of the open field and showed less entrance in the first 5 min of a 30-min open field test compared to WT (Figure 6B). In light–dark box tests, cKO mice tended to spend less time (Figure 6C, left) and enter fewer times (Figure 6C, middle) in the light area, but spent much more time to enter the light box (Figure 6C, right). Moreover, exploration analysis of cKO mice showed less significant entries of open arm in an elevated plus maze than that of WT mice (Figure 6D, left), however, the time in the open arms showed unchanged (Figure 6D, right).

Then we conducted learning and memory tests by using Y maze experiment and Morris Water Maze. The results showed that *Arid1a* loss did not cause any difference in both tests as compared with WT (Figure S2 A–D). We also conducted contextual and cued fear conditioning, and the results showed there was no obvious difference between cKO and WT mice (Figure S2 E-G). Marble burying test and self-grooming were used to test autism-like behaviour, but there was no difference in both tests (Figure S2 H-I). Collectively, these results suggested that deletion of microglial *Arid1a* did not cause autism-like behaviour or learning and memory deficits, but resulted in anxiety-like behaviour.

4 | DISCUSSION

Microglia are thought to play an essential role in the differentiation and maturation of precursors into neurons.[45] However, the molecular mechanisms underlying the contribution of the phenotypic plasticity
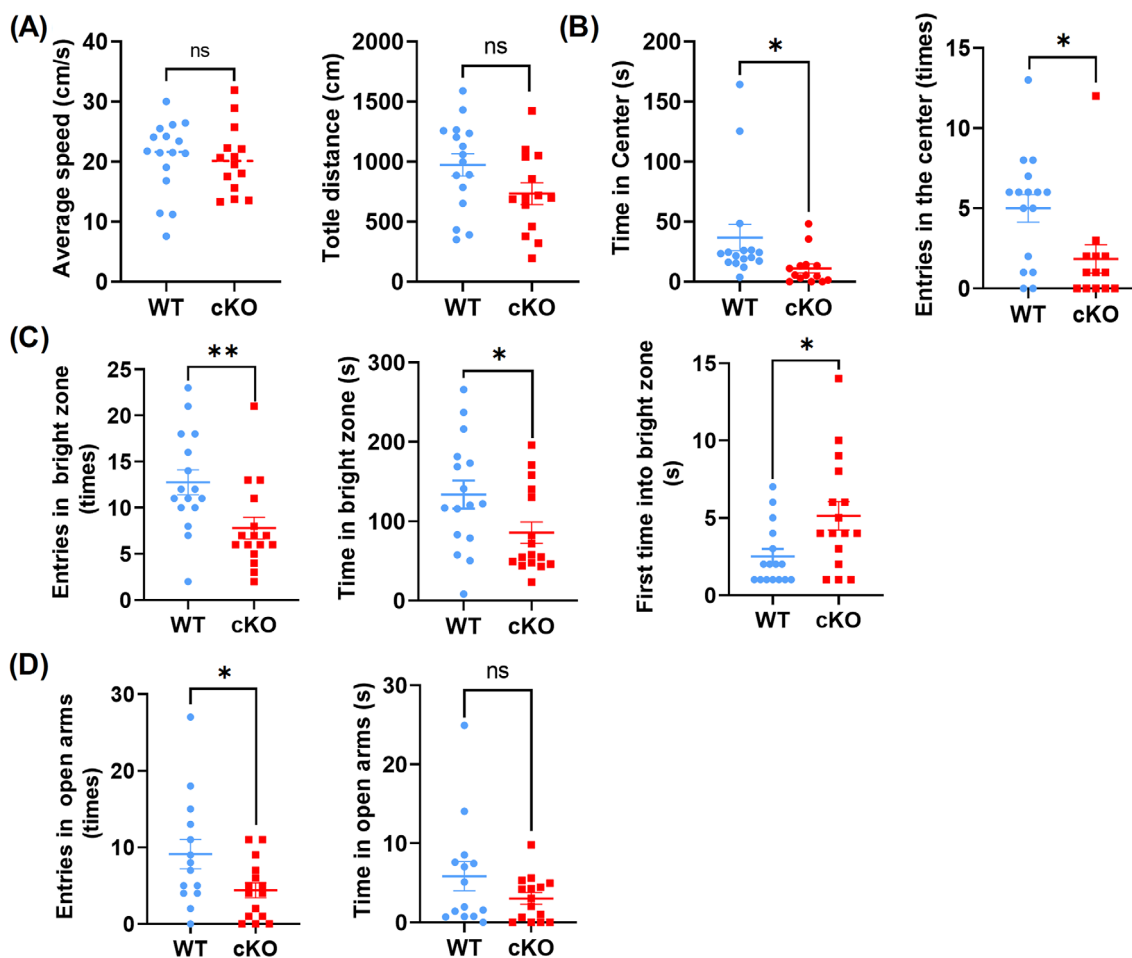
FIGURE 6   Microglial *Arid1a* Absence prior to birth leads to anxiety-like behaviour in mice. (A, B) Open field test of *Arid1a* cKO mice and 6–8-week-old male mice (*n* > 14) were used for open field test, and the average speed (A, left), total distance (A, right), time in centre (B, right), and number of entries to the central area (B, left) were determined. (C) The light–dark transition test. Mice were used as in (A), the numbers of entries to the bright zone (left), the first time into the bright zone (middle), and time in the bright zone were shown (right). (D) Elevated plus maze. Mice were used as in (A), and the number of entries to the open arms (left) and the time spent in the open arms (right) were analysed. Data are expressed as mean ± SEM and analysed by Student's *t*-test, **p* < 0.05 and ***p* < 0.01

of microglia to neurogenesis remain largely unexplored. Here, we leverage microglia-specific *Arid1a* deletion, which altered the dynamic equilibrium of microglial polarization states and caused defective neurogenesis and anxiety-like behaviours, to gain mechanistic insights into the role of chromatin remodelling in the immune capacities of microglia during the development of CNS. This study elaborates the role of chromatin remodelling in governing microglia polarization and the effects of differentially polarized microglia on key functions of NSPCs during neurogenesis.

Classical M1- and M2-polarization states originate from T-helper cell type 1 (Th-1) or T-helper cell type 2 (Th-2) that stimulated peripheral macrophages polarization.[46] Microglia, regarded as CNS residing microphage, have two activation subtypes named M1 and M2, in conformity with the macrophage nomenclature.[47,48] Microglial polarization is one of the most significant features in a variety of CNS disorders such as traumatic brain injury, stroke and many atypical neurogenesis-related diseases.[35,49,50] In our analysis, we found that microglial M1 genes including *Ki*, *Tlr*, *Il1a*, *Il1b*, *Il6*, *Il18* and *Tmem47* significantly increased and M2 genes including *Igf1*, *C1qa*, *Arhgap22*, *Tim47*, *Timp2*, *sema6d* and *fgd2*, significantly changed. Among those M1 genes, aberrant expression of *Il1a*, *Il1b*, *Il6*, *Il18* lead to cells or brain damage,[51] and *Tmem47* plays an important role in M1 microglial migration and could increase the aggregation of M1 microglia at the inflammatory site. M2 genes, including *sema6d* and *Igf1* play important roles in cell development,[52,53] *C1qa* is necessary for microglial phagocytosis,[54] *fgd2* acts as a regulator in leukocyte signalling,[55] which indicates that Arid1a is involved in microglia/microphage polarization balance.

Emerging evidence shows that chromatin remodelling plays an important role in microphage/microglia polarization.[56–58] For example, a histone 3 Lys27 (H3K27) demethylase named Jumonji domain-containing 3 (JMJD3), could activate M2 macrophage development.[59] On the other hand, H3K4me3 enrichment on the promoter of M1 polarization markers, such as IL-6, IL-18, MCP-1 and TNF-α induces long-term inflammation.[60] H3K27ac and H3K4me3 are considered as transcription activation markers,[61,62] and the enrichment of H3K27ac and H3K4me3 on promoters leads to chromatin openness. Previous studies show that ARID1A is involved in H3K27ac modulation and chromatin accessibility.[23,62] Our results further support an essential role of chromatin openness in microglia/microphage polarization. However, whether *Arid1a*-mediated chromatin accessibility crosstalk with these histone modifications in microglia needs further investigation.

In the mouse CNS, *Arid1a* is highly expressed in astrocytes, neurons and microglia,[63] and lack of *Arid1a* in mouse NSPCs or human embryonic stem cells (hESCs) resulted in anomalous neurogenesis, accompanied by an increase of chromatin accessibility enrichment.[24,28] Our use of ATAC-seq allowed us to connect microglia chromatin accessibility to the abnormal polarization pattern of M1/M2 microglia in *Arid1a* cKO mice. This connection, to our knowledge, has not been previously made. Recent studies have shown that polarized microglia have differential effects on the differentiation potential of NSPCs, with M1 microglia inhibiting neurogenesis, while M2 microglia supporting neurogenesis.[35] By showing that M1 microglial polarization was enhanced, but M2 polarization was weakened following microglia-specific *Arid1a* deletion, we observed impairment of neuronal differentiation, but not proliferation, and this is mainly due to Il1a expression enhancement upon *Arid1a* loss. Although Il1a has been reported to stimulate proliferation of NSPCs, however, in our analysis, we found that the expression of Il6, previously demonstrated to inhibit proliferation of NSPCs, was increased after *Arid1a* loss in microglia. Therefore, the concurrent increase of Il1a and Il6 expression after *Arid1a* loss may lead to no effects on NSPCs proliferation.[64]

Increasing evidence suggests that immune cells play important roles in brain development and behaviours. Defects of immune cells, including CD4$^+$ T-cells, Th17/Treg, mast cell and microglia,[41–44] lead to anxiety or anxiety-like behaviours. Recent studies have shown that stimulated M2 polarization intervention enhances neurogenesis and rescues brain damage including brain injury, anxiety and stroke.[65–68] In agreement with an important role of microglia polarization in neurogenesis, our study revealed unbalanced switch of M1/M2 microglial polarization following microglia-specific *Arid1a* deletion, which resulted in deficient neurogenesis both in vivo and in vitro. Il4, regarded as microglial M2 polarization inducible factor, can switch microglial M1/M2 polarization and alleviate neurological damage.[69] Unlike M1 microglia that requires constant stimulation, a single pulsed stimulus with Il4 is sufficient to maintain M2 microglia polarization.[35] In our study, Il4-stimulated M1/M2 polarization switch rescued neurogenesis deficiency induced by *Arid1a* absence in microglia. This is consistent with a recent study in which IL4 overexpression specifically in microglia enhances neurogenesis, in which Il4-stimulated WT microglia can increase both Tuj1+ and GFAP+ cells significantly,[35] and protects mice from stress-induced depressive-like behaviours.[70] Moreover, it has been reported that adult-born neurons are required to buffer stress responses and depressive behaviour,[71] suggesting that enhancement of adult neurogenesis can relieve symptoms of mental illness. Our findings that deficient neurogenesis and anxiety-like behaviours following microglial *Arid1a* deletion was rescued by Il4 stimulation in vivo opened a new avenue of mitigating depressive illness through manipulation of microglial polarization states.

Our data suggest that cellular secretion process, such as cytokine secretion from microglia plays a critical role in modulating neurogenesis. But cellular secretion is a very complicated process. In addition to cytokines, metabolite, microRNA and extracellular vesicle also play irreplaceable role in cell-to-cell mutual regulation.[72–74] One limitation of our study is that we did not examine the effects of metabolites in microglia on neurogenesis. Recent studies have shown that chromatin modifications are intimately tied to metabolic processes.[75] and energy metabolism. Subunits of the SWI/SNF complex are originally identified as transcriptional regulators of genes involved in growth in the presence of alternative fermentable carbon sources, such as sucrose.[76,77] Mammalian SWI/SNF complexes are a family of polybromo-associated BAF complexes, and the subunit Baf60c regulates glycolytic metabolism.[78] Moreover, increasing evidence suggests that metabolic reprogramming plays a key role in innate inflammatory response. Switch of metabolic programme from a growth-encouraging capacity (M2) to a killing/inhibitory capacity (M1) permits

macrophages to respond with appropriate functions under specific conditions.[79,80] For example, when stimulated with LPS, microglia switch from oxidative metabolism toward glycolytic metabolism.[81] Based on our RNA-seq analysis, we found that there was a functional weakness in metabolic biosynthesis (KEGG: mmu00601, mmu00515, and mmu00562, date not shown), and the cKO mice showed a significant body weight loss, which is consistent with previous reports showing that *Arid1a* regulates glutathione and lipid metabolism.[82,83] To extend our findings, future study on the connection between chromatin remodelling, microglia polarization and metabolism is needed.

In conclusion, our studies uncover an unforeseen link between chromatin remodelling, dynamic equilibrium of microglial polarization, and defective neurogenesis and anxiety-like behaviours. Reprogramming microglia polarization states with IL4 can restore deficient neurogenesis caused by *Arid1a* loss in microglia. These results provide a mechanistic insight into the role of chromatin remodelling in microglial biology, and highlight a new direction of mitigating neuropsychiatric disorders through manipulation of the activity of chromatin remodelers.

AUTHOR CONTRIBUTIONS

Maolei Gong and Chang-Mei Liu, conception and design, collection and assembly of data, data analysis and interpretation, manuscript writing, final approval of manuscript; Xiao Liu, Ruoxi Shi, Yijun Liu, Jinpeng Ke, and Hong-Zhen Du, collection and assembly of data.

ACKNOWLEDGEMENTS

CONFLICT OF INTEREST

The authors declare no conflict of interest.

DATA AVAILABILITY STATEMENT

The RNA-seq and ATAC-seq datasets generated and analyzed in this study have been deposited in the NCBI Sequence Read Archive (SRA). The raw data for microglia RNA-seq on p15 extracted using FACS are accessible through the series accession number PRJNA812340 (https://www.ncbi.nlm.nih.gov/bioproject/PRJNA812340/). For primary microglia ATAC-seq are accessible through the series accession number PRJNA 812630 (https://www.ncbi.nlm.nih.gov/bioproject/PRJNA812630/). For mouse Arid1a ChIP-seq accessible through the series accession number PRJNA638150 (https://www.ncbi.nlm.nih.gov/bioproject/PRJNA638150/).

ORCID

Chang-Mei Liu https://orcid.org/0000-0002-2941-4667

REFERENCES

1. Tay TL, Savage JC, Hui CW, Bisht K, Tremblay M. Microglia across the lifespan: from origin to function in brain development, plasticity and cognition. *J Physiol*. 2017;595(6):1929-1945.
2. Mancuso R, van den Daele J, Fattorelli N, et al. Stem-cell-derived human microglia transplanted in mouse brain to study human disease. *Nature Neurosci*. 2019;22(12):2111-2116.
3. Kwon HS, Koh SH. Neuroinflammation in neurodegenerative disorders: the roles of microglia and astrocytes. *Transl Neurodegen*. 2020;9(1):42.
4. Bartels T, De Schepper S, Hong S. Microglia modulate neurodegeneration in Alzheimer's and Parkinson's diseases. *Science (New York, NY)*. 2020;370(6512):66-69.
5. Karve IP, Taylor JM, Crack PJ. The contribution of astrocytes and microglia to traumatic brain injury. *Br J Pharmacol*. 2016;173(4):692-702.
6. Berghoff SA, Spieth L, Sun T, et al. Microglia facilitate repair of demyelinated lesions via post-squalene sterol synthesis. *Nat Neurosci*. 2021;24(1):47-60.
7. Sierra A, Encinas JM, Deudero JJ, et al. Microglia shape adult hippocampal neurogenesis through apoptosis-coupled phagocytosis. *Cell stem cell*. 2010;7(4):483-495.
8. Das S, Narayanan S, Paramasivan CN, Lowrie DB, Narayanan PR. Human tuberculosis sera show prominent antibody responses to particulate fractions of mycobacterium tuberculosis. *J Clin Immunol*. 1991;11(2):74-77.
9. Hanisch UK, Kettenmann H. Microglia: active sensor and versatile effector cells in the normal and pathologic brain. *Nat Neurosci*. 2007;10(11):1387-1394.
10. Ekdahl CT, Claasen JH, Bonde S, Kokaia Z, Lindvall O. Inflammation is detrimental for neurogenesis in adult brain. *Proc Natl Acad Sci U S A*. 2003;100(23):13632-13637.
11. Miron VE, Boyd A, Zhao JW, et al. M2 microglia and macrophages drive oligodendrocyte differentiation during CNS remyelination. *Nat Neurosci*. 2013;16(9):1211-1218.
12. Liu Z, Fan Y, Won SJ, et al. Chronic treatment with minocycline preserves adult new neurons and reduces functional impairment after focal cerebral ischemia. *Stroke*. 2007;38(1):146-152.
13. Zhang Z, Zhang Z, Lu H, Yang Q, Wu H, Wang J. Microglial polarization and inflammatory mediators after intracerebral hemorrhage. *Mol Neurobiol*. 2017;54(3):1874-1886.
14. Wu J, Huang B, Chen H, et al. The landscape of accessible chromatin in mammalian preimplantation embryos. *Nature*. 2016;534(7609):652-657.
15. Ramirez-Carrozzi VR, Braas D, Bhatt DM, et al. A unifying model for the selective regulation of inducible transcription by CpG Islands and nucleosome remodeling. *Cell*. 2009;138(1):114-128.
16. Li B, Carey M, Workman JL. The role of chromatin during transcription. *Cell*. 2007;128(4):707-719.
17. Ribeiro-Silva C, Vermeulen W, Lans H. SWI/SNF: complex complexes in genome stability and cancer. *DNA Repair*. 2019;77:87-95.
18. Jia SJ, Gao KQ, Zhao M. Epigenetic regulation in monocyte/macrophage: a key player during atherosclerosis. *Cardiovasc Ther*. 2017;35(3):e12262.
19. Schmidt SV, Krebs W, Ulas T, et al. The transcriptional regulator network of human inflammatory macrophages is defined by open chromatin. *Cell Res*. 2016;26(2):151-170.
20. Lawrence T, Natoli G. Transcriptional regulation of macrophage polarization: enabling diversity with identity. *Nat Rev Immunol*. 2011;11(11):750-761.
21. Wang W, Côté J, Xue Y, et al. Purification and biochemical heterogeneity of the mammalian SWI-SNF complex. *EMBO J*. 1996;15(19):5370-5382.
22. Ronan JL, Wu W, Crabtree GR. From neural development to cognition: unexpected roles for chromatin. *Nat Rev Genet*. 2013;14(5):347-359.

23. Kelso TWR, Porter DK, Amaral ML, Shokhirev MN, Benner C, Hargreaves DC. Chromatin accessibility underlies synthetic lethality of SWI/SNF subunits in ARID1A-mutant cancers. *Elife*. 2017;6: e30506.

24. Liu J, Liu S, Gao H, et al. Genome-wide studies reveal the essential and opposite roles of ARID1A in controlling human cardiogenesis and neurogenesis from pluripotent stem cells. *Genome Biol*. 2020;21 (1):169.

25. Mehrvarz Sarshekeh A, Alshenaifi J, Roszik J, et al. ARID1A mutation may define an immunologically active subgroup in patients with microsatellite stable colorectal cancer. *Clin Cancer Res*. 2021;27(6): 1663-1670.

26. Slavotinek A, Lefebvre M, Brehin AC, et al. Prenatal presentation of multiple anomalies associated with haploinsufficiency for ARID1A. *Eur J Med Genet*. 2022;65(2):104407.

27. Cowan M, Petri WA Jr. Microglia: immune regulators of neurodevelopment. *Front Immunol*. 2018;9:2576.

28. Liu X, Dai SK, Liu PP, Liu CM. Arid1a regulates neural stem/progenitor cell proliferation and differentiation during cortical development. *Cell Prolif*. 2021;54(11):e13124.

29. Gao X, Tate P, Hu P, Tjian R, Skarnes WC, Wang Z. ES cell pluripotency and germ-layer formation require the SWI/SNF chromatin remodeling component BAF250a. *Proc Natl Acad Sci U S A*. 2008;105 (18):6656-6661.

30. Shang XY, Shi Y, He DD, et al. ARID1A deficiency weakens BRG1-RAD21 interaction that jeopardizes chromatin compactness and drives liver cancer cell metastasis. *Cell Death Dis*. 2021;12 (11):990.

31. Wilsker D, Patsialou A, Zumbrun SD, et al. The DNA-binding properties of the ARID-containing subunits of yeast and mammalian SWI/SNF complexes. *Nucleic Acids Res*. 2004;32(4):1345-1353.

32. Chandler RL, Brennan J, Schisler JC, Serber D, Patterson C, Magnuson T. ARID1a-DNA interactions are required for promoter occupancy by SWI/SNF. *Mol Cell Biol*. 2013;33(2):265-280.

33. Butovsky O, Jedrychowski MP, Moore CS, et al. Identification of a unique TGF-β–dependent molecular and functional signature in microglia. *Nat Neurosci*. 2014;17(1):131-143.

34. Butovsky O, Ziv Y, Schwartz A, et al. Microglia activated by IL-4 or IFN-gamma differentially induce neurogenesis and oligodendrogenesis from adult stem/progenitor cells. *Mol Cell Neurosci*. 2006;31(1): 149-160.

35. Vay SU, Flitsch LJ, Rabenstein M, et al. The plasticity of primary microglia and their multifaceted effects on endogenous neural stem cells in vitro and in vivo. *J Neuroinflammation*. 2018;15(1):226.

36. Fu R, Shen Q, Xu P, Luo JJ, Tang Y. Phagocytosis of microglia in the central nervous system diseases. *Mol Neurobiol*. 2014;49(3):1422-1434.

37. Hill AS, Sahay A, Hen R. Increasing adult hippocampal neurogenesis is sufficient to reduce anxiety and depression-like behaviors. *Neuropsychopharmacology*. 2015;40(10):2368-2378.

38. Tunc-Ozcan E, Peng C-Y, Zhu Y, Dunlop SR, Contractor A, Kessler JA. Activating newborn neurons suppresses depression and anxiety-like behaviors. *Nat Commun*. 2019;10(1):3768.

39. Anacker C, Hen R. Adult hippocampal neurogenesis and cognitive flexibility - linking memory and mood. *Nat Rev Neurosci*. 2017;18(6): 335-346.

40. Evonuk KS, Prabhu SD, Young ME, DeSilva TM. Myocardial ischemia/reperfusion impairs neurogenesis and hippocampal-dependent learning and memory. *Brain Behav Immun*. 2017;61:266-273.

41. Nicoloro-SantaBarbara J, Carroll J, Lobel M. Coping, social support, and anxiety in people with mast cell disorders. *Ann Allergy Asthma Immunol*. 2021;127(4):435-440.

42. Fan KQ, Li YY, Wang HL, et al. Stress-induced metabolic disorder in peripheral CD4(+) T cells leads to anxiety-like behavior. *Cell*. 2019; 179(4):864-879.e819.

43. Westfall S, Caracci F, Zhao D, et al. Microbiota metabolites modulate the T helper 17 to regulatory T cell (Th17/Treg) imbalance promoting resilience to stress-induced anxiety- and depressive-like behaviors. *Brain Behav Immun*. 2021;91:350-368.

44. Wang Y-L, Han Q-Q, Gong W-Q, et al. Microglial activation mediates chronic mild stress-induced depressive- and anxiety-like behavior in adult rats. *J Neuroinflammation*. 2018;15(1):21.

45. Aarum J, Sandberg K, Haeberlein SL, Persson MA. Migration and differentiation of neural precursor cells can be directed by microglia. *Proc Natl Acad Sci U S A*. 2003;100(26):15983-15988.

46. Stein M, Keshav S, Harris N, Gordon S. Interleukin 4 potently enhances murine macrophage mannose receptor activity: a marker of alternative immunologic macrophage activation. *J Exp Med*. 1992;176 (1):287-292.

47. Michelucci A, Heurtaux T, Grandbarbe L, Morga E, Heuschling P. Characterization of the microglial phenotype under specific proinflammatory and anti-inflammatory conditions: effects of oligomeric and fibrillar amyloid-beta. *J Neuroimmunol*. 2009;210(1–2):3-12.

48. Kreutzberg GW. Microglia: a sensor for pathological events in the CNS. *Trends Neurosci*. 1996;19(8):312-318.

49. Wu H, Zheng J, Xu S, et al. Mer regulates microglial/macrophage M1/M2 polarization and alleviates neuroinflammation following traumatic brain injury. *J Neuroinflammation*. 2021;18(1):2.

50. Ye SY, Apple JE, Ren X, et al. Microglial VPS35 deficiency regulates microglial polarization and decreases ischemic stroke-induced damage in the cortex. *J Neuroinflammation*. 2019;16(1):235.

51. Misener VL, Gomez L, Wigg KG, et al. Cytokine genes TNF, IL1A, IL1B, IL6, IL1RN and IL10, and childhood-onset mood disorders. *Neuropsychobiology*. 2008;58(2):71-80.

52. Thomas T, Perdue MV, Khalaf S, et al. Neuroimaging genetic associations between SEMA6D, brain structure, and reading skills. *J Clin Exp Neuropsychol*. 2021;43(3):276-289.

53. Netchine I, Azzi S, Le Bouc Y, Savage MO. IGF1 molecular anomalies demonstrate its critical role in fetal, postnatal growth and brain development. *Best Pract Res Clin Endocrinol Metab*. 2011;25(1):181-190.

54. Lui H, Zhang J, Makinson SR, et al. Progranulin deficiency promotes circuit-specific synaptic pruning by microglia via complement activation. *Cell*. 2016;165(4):921-935.

55. Huber C, Mårtensson A, Bokoch GM, Nemazee D, Gavin AL. FGD2, a CDC42-specific exchange factor expressed by antigen-presenting cells, localizes to early endosomes and active membrane ruffles. *J Biol Chem*. 2008;283(49):34002-34012.

56. Przanowski P, Mondal SS, Cabaj A, et al. Open chromatin landscape of rat microglia upon proinvasive or inflammatory polarization. *Glia*. 2019;67(12):2312-2328.

57. Van den Bossche J, Neele AE, Hoeksema MA, de Winther MP. Macrophage polarization: the epigenetic point of view. *Curr Opin Lipidol*. 2014;25(5):367-373.

58. Schultze JL. Chromatin remodeling in monocyte and macrophage activation. *Adv Protein Chem Struct Biol*. 2017;106:1-15.

59. Satoh T, Takeuchi O, Vandenbon A, et al. The Jmjd3-Irf4 axis regulates M2 macrophage polarization and host responses against helminth infection. *Nat Immunol*. 2010;11(10):936-944.

60. Bekkering S, Quintin J, Joosten LA, van der Meer JW, Netea MG, Riksen NP. Oxidized low-density lipoprotein induces long-term proinflammatory cytokine production and foam cell formation via epigenetic reprogramming of monocytes. *Arterioscler Thromb Vasc Biol*. 2014;34(8):1731-1738.

61. Howe FS, Fischl H, Murray SC, Mellor J. Is H3K4me3 instructive for transcription activation? *BioEssays*. 2017;39(1):1-12.

62. Roth SY, Denu JM, Allis CD. Histone acetyltransferases. *Annu Rev Biochem*. 2001;70:81-120.

63. Zhang Y, Chen K, Sloan SA, et al. An RNA-sequencing transcriptome and splicing database of glia, neurons, and vascular cells of the cerebral cortex. *J Neurosci*. 2014;34(36):11929-11947.

64. McPherson CA, Aoyama M, Harry GJ. Interleukin (IL)-1 and IL-6 regulation of neural progenitor cell proliferation with hippocampal injury: differential regulatory pathways in the subgranular zone (SGZ) of the adolescent and mature mouse brain. *Brain Behav Immun*. 2011;25(5):850-862.

65. Yang Y, Ye Y, Kong C, et al. MiR-124 enriched exosomes promoted the M2 polarization of microglia and enhanced hippocampus neurogenesis after traumatic brain injury by inhibiting TLR4 pathway. *Neurochem Res*. 2019;44(4):811-828.

66. Li L, Gan H, Jin H, et al. Astragaloside IV promotes microglia/macrophages M2 polarization and enhances neurogenesis and angiogenesis through PPARγ pathway after cerebral ischemia/reperfusion injury in rats. *Int Immunopharmacol*. 2021;92:107335.

67. Zhang J, Xie X, Tang M, et al. Salvianolic acid B promotes microglial M2-polarization and rescues neurogenesis in stress-exposed mice. *Brain Behav Immun*. 2017;66:111-124.

68. Xiao L, Wei F, Zhou Y, et al. Dihydrolipoic acid-gold nanoclusters regulate microglial polarization and have the potential to Alter neurogenesis. *Nano Lett*. 2020;20(1):478-495.

69. He Y, Gao Y, Zhang Q, Zhou G, Cao F, Yao S. IL-4 switches microglia/macrophage M1/M2 polarization and alleviates neurological damage by modulating the JAK1/STAT6 pathway following ICH. *Neuroscience*. 2020;437:161-171.

70. Zhang J, Rong P, Zhang L, et al. IL4-driven microglia modulate stress resilience through BDNF-dependent neurogenesis. *Science (New York, NY: Online)*. 2021;7(12):eabb9888.

71. Snyder JS, Soumier A, Brewer M, Pickel J, Cameron HA. Adult hippocampal neurogenesis buffers stress responses and depressive behaviour. *Nature*. 2011;476(7361):458-461.

72. Funcke JB, Scherer PE. Beyond adiponectin and leptin: adipose tissue-derived mediators of inter-organ communication. *J Lipid Res*. 2019;60(10):1648-1684.

73. Mohr AM, Mott JL. Overview of microRNA biology. *Semin Liver Dis*. 2015;35(1):3-11.

74. Nieland L, Morsett LM, Broekman MLD, Breakefield XO, Abels ER. Extracellular vesicle-mediated bilateral communication between glioblastoma and astrocytes. *Trends Neurosci*. 2021;44(3):215-226.

75. Gut P, Verdin E. The nexus of chromatin regulation and intermediary metabolism. *Nature*. 2013;502(7472):489-498.

76. Stern M, Jensen R, Herskowitz I. Five SWI genes are required for expression of the HO gene in yeast. *J Mol Biol*. 1984;178(4):853-868.

77. Neigeborn L, Carlson M. Genes affecting the regulation of SUC2 gene expression by glucose repression in Saccharomyces cerevisiae. *Genetics*. 1984;108(4):845-858.

78. Meng ZX, Li S, Wang L, et al. Baf60c drives glycolytic metabolism in the muscle and improves systemic glucose homeostasis through Deptor-mediated Akt activation. *Nat Med*. 2013;19(5):640-645.

79. Mills CD. M1 and M2 macrophages: oracles of health and disease. *Crit Rev Immunol*. 2012;32(6):463-488.

80. Biswas SK, Mantovani A. Orchestration of metabolism by macrophages. *Cell Metab*. 2012;15(4):432-437.

81. Gimeno-Bayón J, López-López A, Rodríguez MJ, Mahy N. Glucose pathways adaptation supports acquisition of activated microglia phenotype. *J Neurosci Res*. 2014;92(6):723-731.

82. Qu YL, Deng CH, Luo Q, et al. Arid1a regulates insulin sensitivity and lipid metabolism. *EBioMedicine*. 2019;42:481-493.

83. Ogiwara H, Takahashi K, Sasaki M, et al. Targeting the vulnerability of glutathione metabolism in ARID1A-deficient cancers. *Cancer Cell*. 2019;35(2):177-190.e178.

SUPPORTING INFORMATION

Additional supporting information can be found online in the Supporting Information section at the end of this article.